ARL-TR-10106 ● May 2025

RF Hardware Adaptive Filter Design for Reducing RF Interference in UWB SAR Systems

by Benjamin Kirk, Justin Rossler, Emma Lever, Alex Bouvy, Kyle Gallagher, Austin Egbert, Charles Baylis, and Robert Marks

NOTICES

Disclaimers

ARL-TR-10106 ● MAY 2025

RF Hardware Adaptive Filter Design for Reducing RF Interference in UWB SAR Systems

Benjamin Kirk, Alex Bouvy, and Kyle Gallagher
DEVCOM Army Research Laboratory

Justin Rossler, Emma Lever, Austin Egbert, Charles Baylis, and Robert Marks
Baylor University

REPORT DOCUMENTATION PAGE

1. REPORT DATE	2. REPORT TYPE	3. DATES COVERED START DATE	3. DATES COVERED END DATE
May 2025	Technical Report	July 1, 2022	December 1, 2024

4. TITLE AND SUBTITLE
RF Hardware Adaptive Filter Design for Reducing RF Interference in UWB SAR Systems

5a. CONTRACT NUMBER	5b. GRANT NUMBER	5c. PROGRAM ELEMENT NUMBER
5d. PROJECT NUMBER	**5e. TASK NUMBER**	**5f. WORK UNIT NUMBER**

6. AUTHOR(S)
Benjamin Kirk, Justin Rossler, Emma Lever, Alex Bouvy, Kyle Gallagher, Austin Egbert, Charles Baylis, and Robert Marks

7. PERFORMING ORGANIZATION NAME(S) AND ADDRESS(ES)	8. PERFORMING ORGANIZATION REPORT NUMBER
DEVCOM Army Research Laboratory ATTN: FCDD-RLA-LC Adelphi, MD 20783	ARL-TR-10106

9. SPONSORING/MONITORING AGENCY NAME(S) AND ADDRESS(ES)	10. SPONSOR/MONITOR'S ACRONYM(S)	11. SPONSOR/MONITOR'S REPORT NUMBER(S)

12. DISTRIBUTION/AVAILABILITY STATEMENT
DISTRIBUTION STATEMENT A. Approved for public release: distribution unlimited.

13. SUPPLEMENTARY NOTES

14. ABSTRACT
Ultrawide bandwidth (UWB) synthetic aperture radar (SAR) requires access to large swaths of the electromagnetic spectrum (EMS) to perform high-resolution imaging of targets of interest. This large swath of spectrum should begin in the very-high-frequency to lower ultra-high-frequency band to provide the SAR system with obstacle penetration. This portion of the spectrum has become increasingly congested with the proliferation of commercial wireless technologies and the increased need for high-throughput DoD communications systems. This results in the UWB SAR system incurring significant interference while operating in overlapping bands with these other systems. The spectrum changes dynamically with geolocation as well as time. An RF filtering solution is required to alleviate this interference. In conjunction with spectrum situational awareness, this filter will allow the SAR system to adapt to a changing EMS and maintain its performance for target detection. The state of the art both in commercially available devices and the research community is explored, but a solution with the low-loss, high-linearity, operating frequency coverage, and number of notches was not found. In this work, we address this problem through the design of an adaptable RF notch filter.

15. SUBJECT TERMS
Electromagnetic Spectrum Sciences, adaptive filter, radio frequency interference, ultra-wideband radar, notch filter, microwave circuit, high linearity

16. SECURITY CLASSIFICATION OF: a. REPORT	b. ABSTRACT	C. THIS PAGE	17. LIMITATION OF ABSTRACT	18. NUMBER OF PAGES
UNCLASSIFIED	UNCLASSIFIED	UNCLASSIFIED	UU	28

19a. NAME OF RESPONSIBLE PERSON	19b. PHONE NUMBER *(Include area code)*
Benjamin Kirk	(301) 394-3172

STANDARD FORM 298 (REV. 5/2020)
Prescribed by ANSI Std. Z39.18

Contents

List of Figures **iv**

List of Tables **iv**

1. Introduction and Background **1**

2. Review of the State of the Art for Tunable Notch Filters **3**

2.1 TNF Design for UWB SAR 8

2.2 TNF Optimization and Fabrication 10

3. Measurement Results **11**

4. Conclusions **15**

5. Path Forward **15**

6. References **17**

List of Symbols, Abbreviations, and Acronyms **21**

Distribution List **22**

List of Figures

Figure 1. An example of spectrum waterfall (top) and highlighted congestion spectrum (bottom). Yellow areas illustrate infrequent activity that may require dynamic filtering.. 1

Figure 2. Two radar range profiles are shown on the left. The blue trace shows three clear targets and a lower noise floor than the red trace where only two targets are visible. Similarly, the two SAR images in the center and right show an increased noise floor when RFI is present............... 2

Figure 3. Cognitive notching filter design concept. 2

Figure 4. Radar RX chain incorporated with a TNF. 3

Figure 5. Reflective vs. absorptive TNF comparison: power flow through radar RX chain for desired power (green) and interferer power (red) (no ghost target in absorptive TNF). 4

Figure 6. Illustration of decade-BW TNF layout using a 50-transmission line, MEMS switches, inductors, capacitors, and open-circuit resonators. .. 9

Figure 7. Fabricated TNF design... 10

Figure 8. Measurement setup to characterize the TNF S-parameter performance. 12

Figure 9. Simulated (dash) and measured (solid) S_{21} of the TNF for every state (independently switchable) with a single-pole notch from 400 to 4000 MHz. 12

Figure 10. Simulated (dash) and measured (solid) S_{21} of the TNF for every state (independently switchable) with a dual-pole notch from 400 to 4000 MHz. 12

List of Tables

Table 1. Typical TNF performance within the literature and the COTS market. 6

Table 2. Tunable notch filter comparison. 14

1. Introduction and Background

The electromagnetic spectrum (EMS), and especially the radio frequency (RF) spectrum, are continuously becoming more congested with signals. The high demand for wireless devices from television and radio stations to cell phone use has placed high demand on access to more RF bandwidth (BW) throughout the EMS. All this congestion has made it difficult for some more sensitive systems, such as radar, to operate with the desired performance. This is because many radar applications have had their bands of operation sold off or they require ultrawide BW (UWB). The spectrum from 0 to 2.5 GHz (Figure 1) shows just how full the spectrum can be with high power emitters.

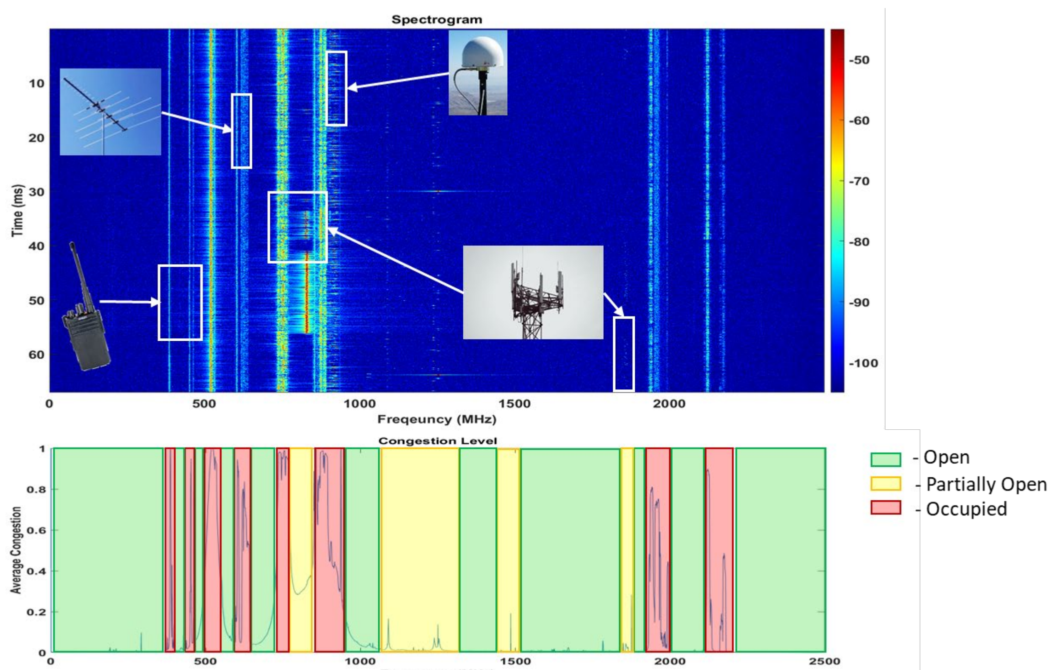

Figure 1. An example of spectrum waterfall (top) and highlighted congestion spectrum (bottom). Yellow areas illustrate infrequent activity that may require dynamic filtering.

A radar operating in this band would suffer from the negative effects of RF interference (RFI) due to spectral collisions with these other signals. RFI will manifest in the form of reduced signal-to-noise plus interference ratio (SINR) at the very least, and it may even cause receiver saturation where data are completely corrupted. In previous and ongoing U.S. Army Combat Capabilities Development Command Army Research Laboratory programs (Office of the Secretary of Defense eSASSY) and in academic literature, researchers have shown that adding a cognitive perception action cycle (PAC) to a radar system that adjusts the radar center frequency and BW can alleviate this degradation in performance from RFI. The cognitive PAC first uses a receiver to sense the RF spectrum and then takes some action based on its observations. Figure 2 shows an example of radar range profiles and synthetic aperture radar (SAR) images with and without RFI avoidance. The reduced sensitivity of the radar without RFI avoidance results in missed targets that are buried in the noise floor.

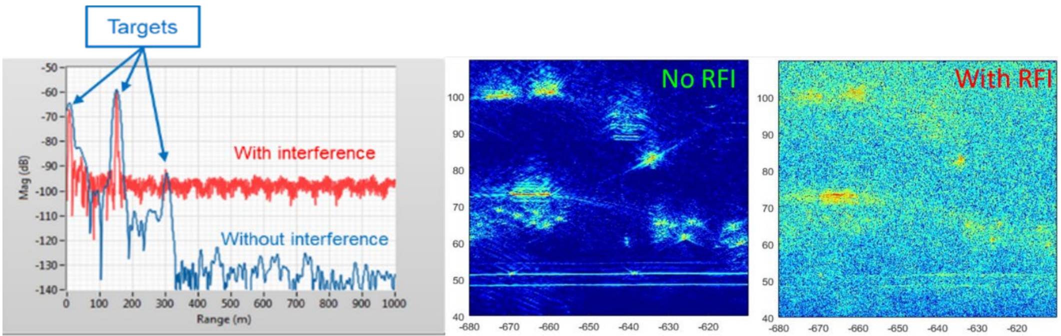

Figure 2. **Two radar range profiles are shown on the left. The blue trace shows three clear targets and a lower noise floor than the red trace where only two targets are visible. Similarly, the two SAR images in the center and right show an increased noise floor when RFI is present.**

For UWB SAR, the problem is even more challenging than previous implementations of PAC with moving target indicator (MTI) radar. UWB SAR radars must cover up to 2 GHz of BW for imaging resolution and have high gain receivers to pick up weak target signatures. This means that high power signals in the RF spectrum will most likely saturate the radar receiver, which will completely corrupt the data obscuring all targets at that time or even damage components of the system. For these reasons, we propose a different approach to the PAC for a UWB SAR system. Figure 3 shows a block diagram where the radar will sense the spectrum, and the action taken will be to tune multiple notch filters to mitigate the RFI before it is passed through the radar front end.

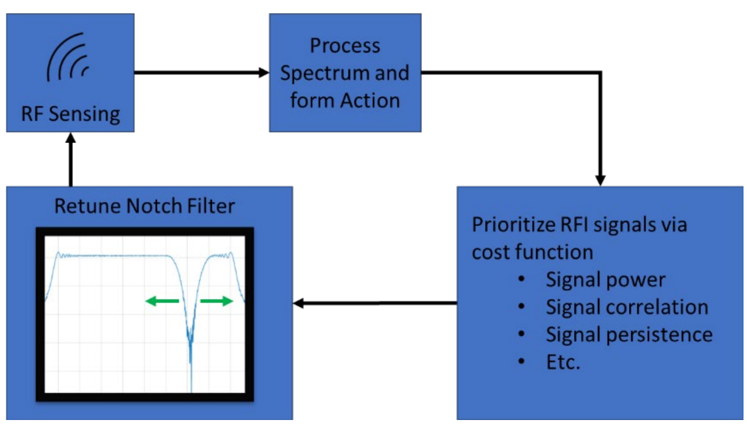

Figure 3. **Cognitive notching filter design concept.**

In this report, we review state of the art for both commercial-off-the-shelf (COTS) available filters and proposed designs in academic literature. In addition, our review establishes the need for a custom design to meet the frequency coverage, linearity, number of notches, and low loss needs of DEVCOM Army Research Laboratory's UWB SAR systems. Furthermore, we develop a custom design that is presented with simulation results and initial measurements of the prototype printed circuit board (PCB). Finally, we present a path forward by outlining the short-term system integration testing and algorithm development for control of the notch filter to react to a changing RF environment.

2. Review of the State of the Art for Tunable Notch Filters

Tunable notch filters (TNFs) may be needed in a radar's receive (RX) chain due to significant dynamic interferers that cause saturation and radar processing problems, which can potentially hinder the sensitivity or dynamic range of the radar. As the spectrum continues to become more congested, due to S-band spectrum reallocations for fifth-generation (5G) wireless communications and other spectrum sell-offs, increased tunability is required. Filters with more notches and greater flexibility in the tunable frequency range of each notch are needed to combat the growing interference spectrum encountered by radar systems. TNFs are typically placed between the RX antenna and the low-noise amplifier (LNA) of a radar RX chain (Figure 4). In the following discussion, we attempt to summarize the state of the art for TNFs.

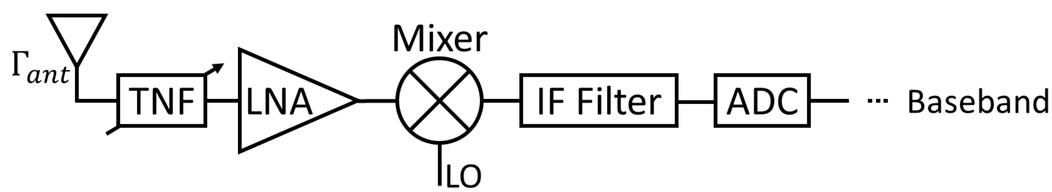

Figure 4. Radar RX chain incorporated with a TNF.

There are two main classes of TNFs in the literature: reflective and absorptive filters. Reflective filters[1–7] reflect power within their stopbands and are more commonly used due to their simpler and more versatile design process. This type of filter can be developed by using either series or shunt resonators, with parallel resonators connected in series and series resonators connected in shunt. At the resonance or "notch" frequency, series resonators act as open circuits, and shunt resonators act as short circuits, and hence reflect the power back out of the filter instead of transmitting the power down the chain. However, some significant radar processing problems can arise because the notched frequency power is reflected into the opposite direction of the traveling wave. Due to the potential for multiple internal amplifier chain reflections in a radar, this may result in a "ghost target" reflection that reaches the analog-to-digital converter (ADC) with a delay, resulting in an identification of an additional, nonexistent target at greater range than the actual target. Since the TNF is often placed as the first element after the RX antenna, this is not always a critical problem because a significant portion of the reflected power can simply be retransmitted back out the antenna if the matching quality is reasonable throughout the circuit. Absorptive filters[8–14] solve the internal reflection problem by using destructive interference to dissipate the interferer power at the notch frequency into the resonator. Absorptive filters achieve this destructive interference by creating a multipath design with a 180° phase shift path at the notch frequency, resulting in theoretically infinite notch depth and complete dissipation of power into the resonators (Figure 5).[8] The filters typically include a delay line and a coupled resonator signal path to achieve the destructive interference and dissipation of power into the resonators. Unlike reflective filters, absorptive filters' resonators are connected by external and interresonator coupling factors,[8] which are also known as coupling coefficients.[14] Thus, the resonator circuitry is connected via the proximity to the main transmission line, and once fabricated, it is fixed in position. Removing an absorptive filter's notch in the passband filter response possesses more design challenges than a reflective filter, since reflective filters can easily implement switchable shunt resonators.[1,5,6]

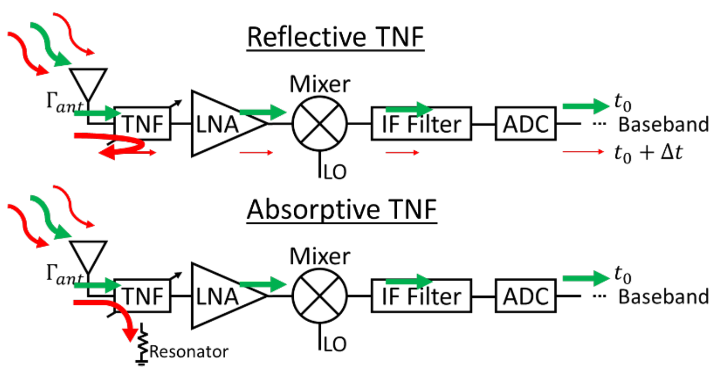

Figure 5. Reflective vs. absorptive TNF comparison: power flow through radar RX chain for desired power (green) and interferer power (red) (no ghost target in absorptive TNF).

The literature has shown TNFs that have between one and four notches, with some possessing independent notch tuning. Although some filter designs achieve significant single-notch tunability using single-pole *N*-throw switched filter banks, other designs strive to harness the capability of notching several interferers simultaneously requiring multi-notch tunable filters. However, the literature shows that, with more notches in a TNF, the notch-tunable BW is increasingly limited. When designing a TNF, the selection of the type of resonator and tunable device is an important part of the design. Many different resonators and tunable devices have been demonstrated in the literature to create a notch filter: series inductor-capacitor (LC) resonators,[1] cascaded low-pass and high-pass filter combinations,[2] stepped impedance resonator,[3] different shaped resonant stubs,[4–7] and others. The selection of these components is important because the quality factor and loss for each component will limit the notch depth and BW, as well as the passband loss of the filter.

Table 1 summarizes the performance of different TNF types as found both in COTS hardware and the literature, and typical TNF performance metrics are discussed. Notch depth[7,10,12,15–21] ranges from 12 to 53 dB with passband loss[6,12,15,16,19–23] ranging from 0.5 to 3 dB. However, many filters achieve passband loss at <1 dB and notch depth at ≥40 dB. High-quality PCB board materials are often used to minimize passband insertion losses. Although it is not often reported, the 3-dB BW[3,15,16] typically ranges from 3% to 7%. These resonators can become tunable by replacing the fixed capacitors with tunable capacitors. There are several options for tunable devices, each with their own benefits and drawbacks, such as the following: varactor diodes,[15,20,21,24] PIN diodes,[15,20,22,23] RF microelectrical mechanical systems (MEMS) capacitors,[4] piezoelectric actuators,[16–18] ferroelectrics, and optical switches.[22] Each tunable notch typically possesses only 1.07:1 to 1.45:1 frequency tuning capabilities.[4,8,10–12,15,20,21,23,24] Absorptive-based filters have been demonstrated to be a viable method of improving notch depth and tunable notch BW. Although varactors and PIN diodes are widely available and have fast switching speeds, they have poor linearity and loss, which makes them nonideal for a TNF design. From the tunable devices demonstrated in the literature, RF MEMS-tunable capacitors are the best components for TNFs placed between the RX antenna and the LNA of a radar's RX chain. RF MEMS-tunable capacitors have a very low insertion loss, very low intermodulation products and harmonics, high-quality factor, high-capacitance tunability, low-power consumption, ability to be integrated on a low dielectric constant (ε_r) substrate, and good reliability (due to the noncontact structure).[25] The drawbacks of using these components are slow switching speeds and limited COTS availability. An important aspect of RF MEMS-tunable capacitors is that their main design trade-off is the inverse relationship of linearity and quality factor and tuning range.[25] Linearity (IIP3) is reported in the literature[22–24] ranging from 10 to 45 dBm. Many papers state that RF MEMS-tunable capacitors provide a significant increase in linearity, insertion loss, and quality factor over varactor and PIN diode technologies. Other topics discussed in TNF design are maintaining passband flatness and correcting for phase changes caused by notching. For optimal flatness, most papers tend toward different designs based on different resonators and resonance techniques.[26] Phase changes are often taken into account by making phase corrections using a phase-locked loop system,[27] phase shifters,[28] and adaptive algorithms.[29]

The COTS market for tunable notch filters is currently limited, because many developments in this technology have not advanced enough yet to reach the market. Our summary of the COTS market is based on online website listings and responses from company sales representatives. There are several single tunable notch filters limited to an octave tuning range capability. Cavity-based notch filters are often used to achieve up to an octave BW of tuning capabilities. The notch depth of the filter typically ranges from 30 to 50 dB.[30–34] The typical passband insertion[30–34] loss ranges from 0.5 to 5 dB, but the sub 1-dB passband insertion loss notch filters are limited to less than 1 GHz operating BW, and they require many cavity sections to achieve this performance. The top two performing options found on the market are Atlanta Micro's AM3139[35] and Wainwright Instruments' WTRCTW8-670-1000-15-30-40SSK.[36] The AM3139 offers a broad BW tunable single notch (2.5–6 GHz) with a 40-dB notch depth, but it is rather lossy with 2.3 dB typical insertion loss in the passband. The Wainwright component offers good passband loss of 0.75 dB (maximum) and a 40-dB notch depth, but it only offers 330 MHz of notch tunability.

Table 1. Typical TNF performance within the literature and the COTS market.

Source	Notches	Passband loss (dB)	Notch depth (dB)	3-dB notch BW (%)	Tunable notch BW	Linearity
Literature	1–4	0.24–3	12–53	3–14	1.07:1–1.70:1	10–45 dBm
[16]	4	0.24–0.53	12–19	≈5	1.70	Not shown
[21]	4	0.47–1.35	47–53	8–12.5	1.32–1.42	28–45 dBm
COTS	1	0.5–5.0	30–50	1–23	1.02:1–2.4:1	Not shown
[35]	1	2.3	40	20	2.40	Not shown
[36]	1	0.75	40	≈4	1.49	Not shown

The only way to procure a tunable multi-notch filter from within the COTS market is to cascade multiple single-notch filters with the lowest feasible passband insertion loss in series. However, this method quickly increases the passband loss to unacceptable levels and is not a viable option for designing a TNF. Alternatively, individual components easily available in the COTS market can be assembled to design an effective TNF using the techniques identified in the literature. The COTS market has an abundant supply of RF low-loss switches, varactors, PIN diodes, inductors, capacitors, as well as other basic components needed to complete a design. Design boards can be easily fabricated by having a PCB manufacturer develop the board. With this, an effective multi-notch absorptive TNF can be designed and fabricated. This fabrication can be performed using both COTS components and components described in the literature, and reasonable performance expectations include >30-dB notch depth, <3-dB passband loss, moderate notch tunability, and, potentially, poor linearity. With the use of RF MEMS-tunable capacitors over common varactors, the design's linearity, loss, and notch tunable BW can be improved. However, achieving these performance metrics across a decade of BW possesses another challenge. A simple way to increase per-notch tunable BW of a design is to implement a switchable notch filter bank.

The literature and COTS market cover a wide range of topics and design on TNFs, but there are some design achievements that are not shown in the state of the art. Because the current project requires a TNF possessing an entire decade of BW (0.4–4.0 GHz), it is difficult to find TNF designs in the literature that directly meet the specifications over this BW. In addition, state-of-the-art TNFs are typically limited to four notches or fewer, and more notches would likely be needed in a TNF with a decade of BW. Although absorptive notch filters are demonstrated, it is difficult to achieve the freedom of controlling how many notches are presented due to their nature of connectivity to the main signal path (delay line) by means of coupling. With a reflective filter, each shunt resonator can be switched ON or OFF by using an RF low-loss, high-linearity switch. This allows great freedom of control in a design. This method will not work in an absorptive filter because the connection is made with the main signal path (delay line) by the proximity of the resonator path to this delay line. Thus, the literature has only shown absorptive notch filter building blocks with one tunable notch.

Hickle and Peroulis[8] showed two of these single-notch absorptive filters cascaded in series. However, this double-notch composite design requires two notches to be present at all times, even if a second notch is not required by the surrounding interference. Finally, perhaps one of the most significant potential innovation areas is the incorporation of impedance matching with filtering. It is important to maintain the optimal input match to the LNA to minimize reflected power in the passband. Any power reflected in the passband frequencies may cause the reflected portion of the desired signal to be lost in the receiver chain or show up later in time on the radar as a ghost target. Thus, incorporating impedance matching with filtering will be able to provide the optimal impedance match for the bandpass filter response, resulting in an optimal signal-to-noise ratio and minimization of ghost targets. These are the best areas of innovation within the state of the art to further advance TNFs.

In summary, tunable notch filters may be needed in a radar's RX chain to block large interferers from saturating the front end of the radar. Reflective TNFs operate by reflecting the unwanted interference power back toward the receiver antenna (input), which is often not of critical concern because the reflected power will be retransmitted if the matching quality is reasonable throughout the circuit. Absorptive TNFs operate by absorbing the unwanted interference power into the resonators using destructive interference and is advantageous when reflections in the RX chain need to be minimized to avoid ghost targets. Typical TNF performance includes the following: a passband loss ranging from 0.5 to 3.0 dB, a notch depth ranging from 12 to 53 dB, a BW_{3dB} ranging from 3% to 7%, and a notch tunable BW ranging from 1.07:1 to 1.45:1. The COTS market is limited to single-notch TNFs, since most of the TNF innovations have not reached the market yet. TNFs in the literature can be innovated by developing a TNF with a decade BW of operation likely requiring greater than four notches and wider notch tunable BW to cover the UWB.

In the following discussion, we summarize the state of the art for TNFs. Although a lot has been demonstrated in the literature across many TNF designs, there are still a lot of innovations to be made to advance this field to a deployable device that can apply to many radar systems. So, the next steps for this project include developing a tunable notch filter prototype that demonstrates many of the characteristics found in the literature while prioritizing linearity and loss across a decade of operating BW. This design will provide innovation to the field and perform notch filtering across an ultrawide operating BW while maintaining typical TNF performance metrics. The long-term trajectory for this project is to innovate TNFs that will incorporate impedance matching and filtering. If this goal is achieved, it will maximize a radar's signal-to-noise ratio and minimize ghost targets by maximizing the transmitted power through the filter. A TNF with these characteristics will also help avoid receiver saturation, ghost targets, and minimize insertion loss while maximizing the dynamic range of the radar.

2.1 TNF Design for UWB SAR

Because potential interferers vary with both time and geography, a reconfigurable notch filter is needed before the LNA to block unwanted power from causing LNA saturation and many other system processing errors. Figure 4 illustrates the placement of this TNF in an RF system RX chain. Because the TNF is the first component after the RX antenna, high linearity and low loss are critical to avoid distortions and information degradation before the signal reaches the LNA. Because high-power interferers may be present in an RF environment, sufficient power handling of a TNF is needed to effectively operate without failure. Thus, effective reconfigurability, high linearity, low loss, and high-power handling are needed in any given TNF design. In addition, narrowband notches with deep notch depths are needed for effective interference rejection.

Our filter was designed for applications in wideband stepped-frequency radars, which are susceptible to interference due to the large operating BW. Significant notch flexibility is needed over the wide BW to maintain a high SINR while avoiding LNA saturation. However, such UWB TNFs with multiple notches are limited in the literature. This TNF was designed to provide significant notch flexibility to the radar receiver front end with deep notch depths and low passband loss across a decade BW (10:1 notch-able BW from 400 to 4000 MHz), using high linearity and high-power handling components.

Figure 6 illustrates the layout of the TNF using a 50 Ω main transmission line, MEMS switches, series LC resonators, and open-circuit resonators. A single-pole, four-throw MEMS switch is capable of independently connecting each throw, thus operating as four single-pole, single-throw switches that share a common pole.[37] By utilizing the MM5130 MEMS-based switch, significantly improved linearity, loss, and power handling can be achieved with this TNF design as opposed to other switching technologies.[38] Due to the large design BW, it is critical to use resonators that will not introduce in-band harmonic notches. The lower third of the operating BW uses series LC resonators because they do not possess harmonic notches and only exhibit the fundamental desired notch response. These resonators correspond to the two switches on the left side of Figure 6. The upper two-thirds of the operating BW uses open-circuit microstrip stub resonators because they possess a higher quality factor for a deeper notch depth. These two resonators are shown on the right side of Figure 6. Open-circuit microstrip stub resonators only possess odd harmonic resonances, whereas short-circuit microstrip stub resonators possess both even and odd harmonic resonances. Thus, a combination of both series LC resonators and open-circuit microstrip stub resonators provide optimal notch responses across the decade BW.

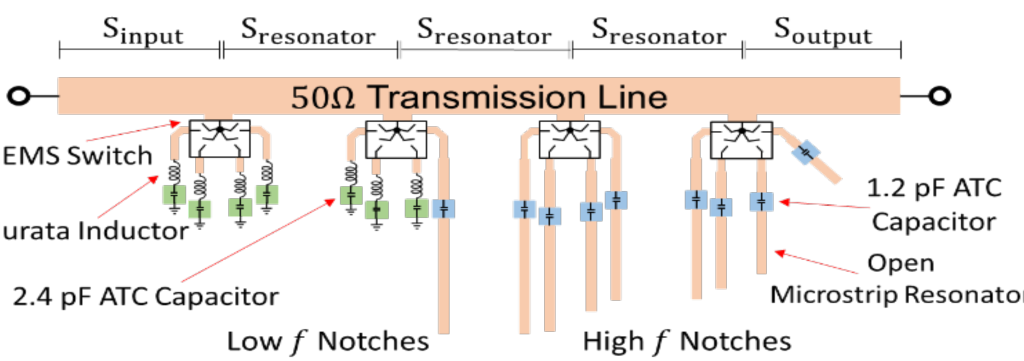

Figure 6. Illustration of decade-BW TNF layout using a 50-transmission line, MEMS switches, inductors, capacitors, and open-circuit resonators.

In addition, capacitors were placed in the middle of the open-circuit microstrip stub resonators to enable manual tuning of the notches to a desired notch frequency. This added capability increases the reliability of the design process and the notch frequency placement flexibility. A notch can be shifted to a desired notch frequency by swapping the nominal 1.2-pF capacitor to another value. In simulation, this capacitor value can shift the realized notch frequency by ±150 MHz.

2.2 TNF Optimization and Fabrication

The TNF design was optimized for 16 independently switchable notches placed across the decade-operating BW of the design, with 8 of the single-pole notches capable of creating 4 dual-pole notches. To finalize the component values and dimensions of the circuit, the Momentum Microwave EM simulation platform was used in conjunction with Advanced Design System (ADS). Modelithics passive component models and commercially provided S-parameter switch data were used to further enhance design analysis. The two-layer board for fabrication has 1.8-mil copper top and bottom layers with a 3-mil Roger RO4003C dielectric. The dielectric possesses 3.55 relative dielectric permittivity and a loss tangent of 0.0027. The simulator was used to choose component values and circuit dimensions to place the fixed, switchable 16 notches as desired throughout the decade BW.

After the design was finalized, the board was prepared for fabrication using KiCad. Since the design uses MEMS switches requiring a high-voltage drive, a control network was developed using a voltage upconverter with the necessary RLC (resistor, inductor, and capacitor) components to switch a 5-V output from an Arduino to an 89-V high-voltage supply for the switches. This supply is fed to each switch gate in the design or ground based on the state of a pull-up transistor switch network. Resistor and capacitor values for this pull-up transistor switch network were calculated to achieve the recommended output voltage and slew rate for the MM5130 switches. The control circuitry and final RF TNF design were placed on a single two-layer board in KiCad and outsourced for fabrication and assembly. Figure 7 shows a photo of the final fabricated TNF.

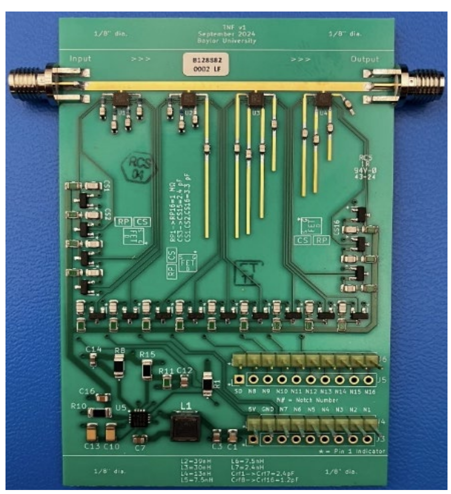

Figure 7. Fabricated TNF design.

3. Measurement Results

The measurement test setup, as shown in Figure 8, consisted of an Arduino Uno to control the state of the TNF, Keysight E5071C Vector Network Analyzer (VNA) to measure the S-parameters, and air-dielectric SMA cables to connect the RF ports of the tuners to the VNA. The VNA was calibrated for a two-port measurement of the TNF design. All 16 single-pole notch responses and all 4 dual-pole notch responses were measured. This characterization spanned across the operating frequency BW of 400–4000 MHz with 3601 data points. Given that each notch can be applied independently of the other notches, any combination of notches can be selected. Adjacent single-pole notch responses can be turned on together for an increased BW of the notch. This scenario may be helpful in rejecting a wide, contiguous range of interferers. For this work, only the single- and dual-pole states are demonstrated. The TNF characterization measurements were completed, and the data are shown in Figures 9 and 10. Figure 9 illustrates the simulated and measured $|S_{21}|$ data of the TNF for every single-pole, single-notch state from 400 to 4000 MHz. Figure 10 shows the simulated and measured $|S_{21}|$ data of the TNF for all 4 dual-pole, single-notch states. To achieve alignment between simulation and measurement results, modifications were made to the manufacturer provided S-parameter model of the switch: an additional series 0.5 Ω resistor was added to each of four switch outputs, and an additional 17-pF capacitor was added to the switch input. Figure 9 shows measured single-pole notch depths that typically achieve between 16 and 25 dB of notch attenuation. Figure 10 shows that even greater attenuation is available with the dual-pole states, which provide between 38 and 46 dB of attenuation, capable of protecting the receiver from stronger interferers. However, an assembly error was found during testing that resulted in a poor connection between the main transmission line and branch 13. This resulted in a reduced notch depth and unreliable performance when this resonator was used. Resolution of this fabrication issue is expected to provide branch 13 with 23 dB single-pole notch depth and near 50 dB dual-pole notch depth when activated with branch 11.

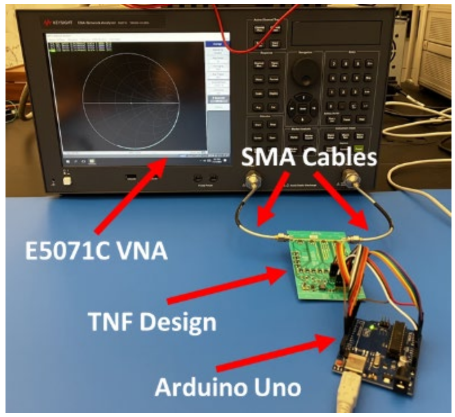

Figure 8. Measurement setup to characterize the TNF S-parameter performance.

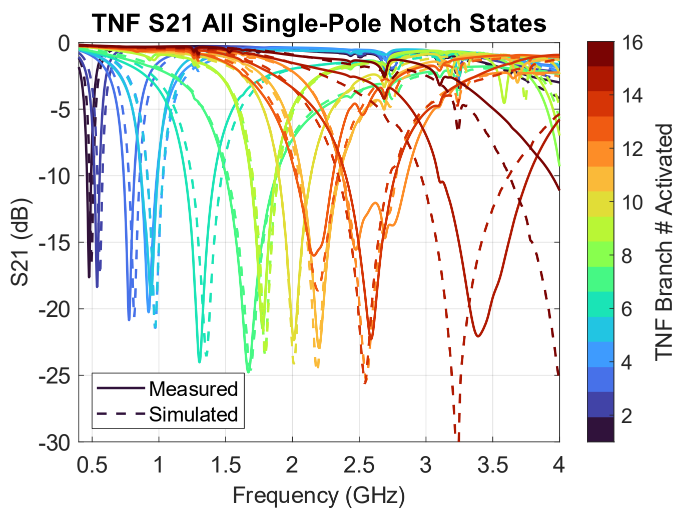

Figure 9. Simulated (dash) and measured (solid) S_{21} of the TNF for every state (independently switchable) with a single-pole notch from 400 to 4000 MHz.

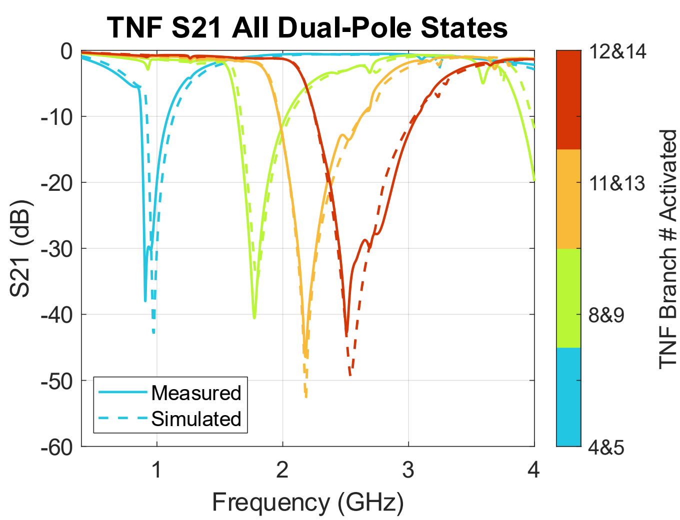

Figure 10. Simulated (dash) and measured (solid) S_{21} of the TNF for every state (independently switchable) with a dual-pole notch from 400 to 4000 MHz.

Table 2 summarizes the performance of the TNF and compares the measurement results with state of the art. The average single-pole notch depth is 21 dB, and the average dual-pole notch depth is 42 dB. Our TNF provides a wider tunable BW than most other contributions in the literature, with the capability to provide more notches. The dual-pole notch setting allows comparable notch depths to those of El-Tanani and Rebeiz[24] while obtaining a wider tunable frequency range.

Table 2. Tunable notch filter comparison.

TNF Design	Ref.	Notches	Passband	Depth	3-dB Notch BW*	Tunable Range	Linearity
Literature (Aggregate)	[3-26]	1-4	0.24 dB - 3.0 dB	12 dB - 53 dB	1.4% - 29%	1.07:1 - 3.63:1	Low - Moderate
1-Pole 4-Notch TNF (Range Focused)	[18]	4	0.24 dB - 0.53 dB	12 dB - 19 dB	1.4% - 1.5%	3.63:1	-
4-Pole 1-Notch Cavity (Range Focused)	[18]	1	0.24 dB - 0.53 dB	30 dB	4.30%	1.70:1	-
4-Pole Stub TNF (Depth Focused)	[24]	2	0.47 dB - 1.35 dB	47 dB - 53 dB	21% - 29%	2.0:1	Moderate
This Work (Single-Pole States)	-	16	0.13 dB - 1.02 dB	16 dB - 25 dB	42.4%	10:1	High
This Work (Dual-Pole States)	-	4	0.13 dB - 1.02 dB	38 dB - 46 dB	51.6%	2.76:1	High

* Calcualated visually from plots

Our notch BW tends to be wider than the comparison systems from the literature in Table 2. The average 3 dB percent BW of all 16 single-pole and 4 dual-pole notches is 44.4%. Since the application for which this filter was designed is a wideband radar receiver, the wider notch response of our design is not concerning. The available notches are spaced throughout the frequency band with an emphasis on the low-end operating frequency band (<2.0 GHz) due to a larger observed tendency for interference at these frequencies. The passband loss of the TNF is also very low, averaging 0.52 dB and achieving as low as 0.13 dB. Furthermore, all but a few frequencies over the decade BW achieve a passband loss less than 1 dB. The MEMS switches and high-current lumped components provide high linearity and high-power handling. Overall, this TNF design provides significant interference rejection flexibility by enabling a narrowband notch to be placed across the decade-tunable BW, whereas providing notch performance and passband loss competitive with the state of the art. The added operating BW without sacrificing interference rejection capabilities provides a significant improvement to wideband receiving systems. These systems can more efficiently operate in a congested spectral environment while rejecting interference and maintaining low receiver noise.

4. Conclusions

In this report, an MEMS-switched, decade BW-TNF for wideband receiver application is demonstrated in design and measurement. The TNF achieves an average passband loss of 0.52 dB, an average single-pole notch depth of 21 dB, an average dual-pole notch depth of 42 dB, and an average 3-dB BW of 44.4%. To our knowledge, this TNF is the first design to achieve a decade-operating BW (10:1) with the capability of placing deep notches and a low passband loss across this broad BW. Single- and double-pole options allow the filter user to trade-off between notch depth and tunable BW. As wideband receiving systems are becoming increasingly affected by the growing spectrum congestion, the filter response can be reconfigured to reject any incoming interference while maintaining a high SINR. Thus, this circuit provides wideband receivers with flexibility to prevent LNA saturation and information degradation in a congested spectral environment.

5. Path Forward

The custom notch filter design and prototype presented in this report will be reprinted with slight modifications to optimize the notch frequency locations. When this updated prototype is received by ARL's academic partner (Baylor University), they will verify the performance with our expected performance. ARL will then verify its performance as well using a VNA. From that point, ARL will begin system integration with loopback benchtop testing to verify the notch filter is effective at amplifier saturation prevention and can be tuned to the desired filter responses via serial interface as needed. In addition, ARL will continue to work with Baylor University to explore more advanced filter designs to further enhance the UWB SAR system's performance.

ARL will work with Baylor University to research, simulate, and test algorithms to automatically choose which notches to activate given spectrum-sensing input from an independent sensing system (such as ARL's SMART and eSASSY nodes) or from the SAR system itself. This will allow completion of the PAC proposed in the problem statement (Figure 3) and involve the evaluation of when notch filtering is necessary based on the interfering signal power level, duty cycle, and modulation. The best algorithm may depend on the exact radar mission and operating environment.

Finally, the filter hardware and spectrum sensing will be integrated in a closed loop to demonstrate the benefit to radar performance in a congested RF environment on the benchtop and over the air. Initially, this will be done with a human in the loop in place of the filter control algorithm. Then, this will be done with the filter control algorithms as well and compared with the baseline system performance without the filtering to show how UWB SAR performance is improved.

6. References

1. Sepidband P, Entesari K. A CMOS UWB receiver with reconfigurable notch filters for narrow-band interferers. 2017 IEEE Radio Frequency Integrated Circuits Symposium; 2017 June 4–6; Honolulu, HI. p. 356359.

2. Gomez-Garcia R, Alonso JI. Systematic method for the exact synthesis of ultra-wideband filtering responses using high-pass and low-pass sections. IEEE Trans Microw Theor Tech. 2006;54(10):3751–3764.

3. Wei F, Chen L, Shi X-W, Liu B. Compact UWB bandpass filter with tunable notch band based on folded SIR. IET Electron Lett. 2011;47(22):1229–1230.

4. Nosrati M, Vahabisani N, Daneshmand M. A novel ultra wideband (UWB) filter with double tunable notch-bands using MEMS capacitors. 2013 IEEE MTT-S International Microwave Symposium; 2013 June 2–7; Seattle, WA.

5. Srivastava R, Pandey AK, Chauhan RK. Design of ultra-wideband filter with reconfigurable notches. 2016 International Conference on Emerging Trends in Communication Technologies (ETCT); 2016 Nov 18–19; Dehradun, India.

6. Bruster A et al. Tunable notch response for ultra wide-band bandpass filter. 2015 IEEE International Conference on Control System, Computing and Engineering (ICCSCE); 2015; Penang, Malaysia. p. 492–497. https://doi.org/10.1109/ICCSCE.2015.7482235

7. Mutalib MA, Zakaria Z, Shairi NA. Electronically tunable transmission zeros bandpass filter with notch response. 2018 18th International Symposium on Antenna Technology and Applied Electromagnetics (ANTEM); 2018; Waterloo, ON, Canada. p. 1–3. https://doi.org/10.1109/ANTEM.2018.8572844

8. Hickle MD, Peroulis D. Theory and design of frequency-tunable absorptive bandstop filters. IEEE Trans Circuits Syst I: Regul Pap. 2018;65(6):1862–1874. https://doi.org/10.1109/TCSI.2017.2766206

9. Psychogiou D, Gomez-Garcia R, Peroulis D. RF-design of narrowband absorptive bandstop filters for UHF applications. 2015 IEEE 16th Annual Wireless and Microwave Technology Conference; 2015 Apr 13–15; Cocoa Beach, FL.

10. Psychogiou D, Gómez-García R, Peroulis D. Wide-passband filters with in-band tunable notches for agile multi-interference suppression in broad-band antenna systems. 2018 IEEE Radio and

Wireless Symposium (RWS); 2018; Anaheim, CA. p. 213–216. https://doi.org/10.1109/10.1109/RWS.2018.8304990

11. Cho Y-H, Park C, Yun S-W. 4-pole tunable absorptive bandstop filters using folded coupled-lines with an inductor. IEEE Access. 2022;10:120191–120199. https://doi.org/10.1109/10.1109/ACCESS.2022.3221461

12. Psychogiou D, Gomez-Garcia R, Peroulis D. Signal-interference bandpass filters with dynamic in-band interference suppression. 2016 IEEE Radio and Wireless Symposium (RWS); 2016; Austin, TX. p. 80–83. https://doi.org/10.1109/10.1109/RWS.2016.7444371

13. Psychogiou D, Gómez-García R, Peroulis D. Recent advances in reconfigurable microwave filter design. 2016 IEEE 17th Annual Wireless and Microwave Technology Conference (WAMICON); 2016; Clearwater, FL. p. 1–6. https://doi.org/10.1109/WAMICON.2016.7483863

14. Snow T, Lee J, Chappell WJ. Tunable high quality-factor absorptive bandstop filter design. 2012 IEEE/MTT-S International Microwave Symposium Digest; 2012; Montreal, QC, Canada. p. 1–3. https://doi.org/10.1109/MWSYM.2012.6259759

15. Song K et al. Compact wide-frequency tunable filter with switchable bandpass and bandstop frequency response. IEEE Access. 2019;7:47503–47508. https://doi.org/10.1109/ACCESS.2019.2908453

16. Naglich EJ, Lee J, Peroulis D, Chappell WJ. High-Q tunable bandstop filters with adaptable bandwidth and pole allocation. 2011 IEEE MTT-S International Microwave Symposium; 2011; Baltimore, MD. p. 1–4. https://doi.org/10.1109/MWSYM.2011.5972936

17. Naglich EJ, Lee J, Peroulis D, Chappell WJ. Switchless tunable bandstop-to-all-pass reconfigurable filter. IEEE Trans Microw Theory Techn. 2012;60(5):1258–1265. https://doi.org/10.1109/TMTT.2012.2188723

18. Naglich EJ, Guyette AC, Peroulis D. High-Q intrinsically-switched quasi-absorptive tunable bandstop filter with electrically-short resonators. 2014 IEEE MTT-S International Microwave Symposium (IMS2014); 2014; Tampa, FL. p. 1–4. https://doi.org/10.1109/MWSYM.2014.6848516

19. Chakraborty P, Shome PP, Panda JR, Deb A. Highly selective UWB bandpass filter with multi-notch characteristics using comb shaped resonator. Prog Electromagn Res M. 2002;108;89–101.

20. Kurra L, Abegaonkar MP, Basu A, Koul SK. Switchable and tunable notch in ultra-wideband filter using electromagnetic bandgap structure. IEEE Microw Wireless Compon Lett. 2014;24(12):839–841. https://doi.org/10.1109/LMWC.2014.2363020

21. Cho Y-H, Rebeiz GM. Tunable 4-pole dual-notch filters for cognitive radios and carrier aggregation systems. IEEE Trans Microw Theor Techn. 2015;63(4):1308–1314. https://doi.org/10.1109/TMTT.2015.2406706

22. Rabbi K, Athukorala L, Panagamuwa CJ, Vardaxoglou JC, Budimir D. High-linearity reconfigurable microstrip UWB bandpass filters. 2011 6th European Microwave Integrated Circuit Conference; 2011 Oct 10–12; Manchester, UK. p. 172–175.

23. Wong PW, Hunter IC. A new class of low-loss high-linearity electronically reconfigurable microwave filter. IEEE Trans Microw Theor Techn. 2008;56(8):1945–1953. https://doi.org/10.1109/TMTT.2008.927395

24. El-Tanani MA, Rebeiz GM. A two-pole two-zero tunable filter with improved linearity. IEEE Trans Microw Theor Techn. 2009;57(4):830–839. https://doi.org/10.1109/TMTT.2009.2015124

25. Khan F, Younis MI. RF MEMS electrostatically actuated tunable capacitors and their applications: a review. J Micromech Microeng. 2021;32(1). https://doi.org/10.1088/1361-6439/ac3cd5

26. Eskandari AR, Kheirdoost A, Haghparast M. Improvement of passband flatness for a compact, narrowband, and highly selective TM dual-mode filter. IEEE Trans Microw Theor Techn. 2020;68(4):1591–1597. https://doi.org/10.1109/TMTT.2019.2963662

27. Silani A, Askari J. A new adaptive phase shifter based on notch filtering and phase-locked loop for measuring the phase margin of a plant. Electrical Engineering (ICEE), Iranian Conference on; 2018; Mashhad, Iran. p. 806–810. https://doi.org/10.1109/ICEE.2018.8472537

28. Kaszynski R, Piskorowski J. Dynamic compensation of phase distortion in time-varying Butterworth filters. 2006 IEEE Instrumentation and Measurement Technology Conference Proceedings; 2006; Sorrento, Italy. p. 1421–1424. https://doi.org/10.1109/IMTC.2006.328600

29. Ekiz O, Constantinides AG. Phase linearity in polyphase filters. 2000 IEEE International Conference on Acoustics, Speech, and Signal Processing. Proceedings (cat. no. 00CH37100); 2000; Istanbul, Turkey. p. 321–323, vol. 1. https://doi.org/10.1109/ICASSP.2000.861959

30. Tunable filters. Atlanta Micro, Inc.; c2025 [accessed 2023 Oct 3]. https://www.atlantamicro.com/filters-old/

31. Tunable notch filters. Ranatec; n.d. [accessed 2023 Oct 3]. https://ranatec.com/tunable-notch-filter/

32. Manually tunable notch filters. Wainwright Instruments; c2018 [accessed 2023 Oct 3]. https://www.wainwright-filters.com/standard-filters/manually-tunable-band-reject-notch-filters

33. Tunable notch filters. Fairview Microwave; n.d. [accessed 2023 Oct 3]. https://www.fairviewmicrowave.com/tunable-band-stop-filters-notch-filters-category.aspx

34. Tunable bandpass and band reject filters. Pasternack; n.d. [accessed 2023 Oct 3]. https://www.pasternack.com/tunable-filters-category.aspx

35. AM3139 FILTER BANK. Atlanta Micro; c2025 [accessed 2023 Oct 3]. https://www.atlantamicro.com/products/filters/am3139/

36. WTRCTW8-670-1000-15-30-40SSK. Wainwright Instruments; c2018 [accessed 2023 Oct 3]. https://www.wainwright-filters.com/application/mobile-communication/5g-nr/wtrctw8-670-1000-330-15-40-075-75-quote/437

37. MM5130 DC to 26 GHz RF switch product overview description [datasheet]. Menlo Microsystems, Inc.; c2025 [accessed 2023 Oct 22]. https://menlomicro.com/images/general/Menlo_MM5130_Datasheet_v2.7.pdf

38. Rebeiz GM et al. Tuning in to RF MEMS. IEEE Microw Mag. 2009;10(6):55–72. https://doi.org/10.1109/MMM.2009.933592

List of Symbols, Abbreviations, and Acronyms

5G	fifth-generation
ADC	analog-to-digital converter
ADS	Advanced Design System
ARL	Army Research Laboratory
BW	bandwidth
COTS	commercial-off-the-shelf
DEVCOM	U.S. Army Combat Capabilities Development Command
DoD	Department of Defense
EM	electromagnetic
EMS	electromagnetic spectrum
LC	inductor-capacitor
LNA	low-noise amplifier
MEMS	microelectrical mechanical systems
MTI	moving target indicator
PAC	perception action cycle
PCB	printed circuit board
RF	radio frequency
RFI	radio frequency interference
RLC	resistor, inductor, and capacitor
RX	receive
SAR	synthetic aperture radar
SINR	signal-to-noise plus interference ratio
TNF	tunable notch filter
UWB	ultrawide bandwidth
VNA	Vector Network Analyzer

1 (PDF)	DEFENSE TECHNICAL INFORMATION CTR DTIC OCA
1 (PDF)	DEVCOM ARL FCDD RLB CI TECH LIB